ADVANCED MATERIALS

Supporting Information

for *Adv. Mater.*, DOI: 10.1002/adma.201601991

Isoelectronic Tungsten Doping in Monolayer $MoSe_2$ for Carrier Type Modulation

*Xufan Li, Ming-Wei Lin, Leonardo Basile, Saban M. Hus, Alexander A. Puretzky, Jaekwang Lee, Yen-Chien Kuo, Lo-Yueh Chang, Kai Wang, Juan C. Idrobo, An-Ping Li, Chia-Hao Chen, Christopher M. Rouleau, David B. Geohegan, and Kai Xiao**

Supporting Information

for

Isoelectronic tungsten doping in monolayer $MoSe_2$ for carrier type modulation

Xufan Li, Ming-Wei Lin, Leonardo Basile, Saban M. Hus, Alexander A. Puretzky, Jaekwang Lee, Yen-Chien Kuo, Lo-Yeuh Chang, Kai Wang, Juan C. Idrobo, An-Ping Li, Chia-Hao Chen, Christopher M. Rouleau, David B. Geohegan, and Kai Xiao

Experimental Methods

Synthesis. The monolayer $MoSe_2$ and $Mo_{1-x}W_xSe_2$ flakes were synthesized though a CVD method conducted in a tube furnace system equipped with a 2" quartz tube. In a typical run, the growth substrates, e.g., Si with 250 nm SiO_2 (SiO_2/Si) or fused quartz plates cleaned by acetone and isopropanol (IPA), were placed face-down above an alumina crucible containing ~0.2 g of MoO_3 powder (for the growth of $Mo_{1-x}W_xSe_2$, a mixture of MoO_3 and WO_3 powder was used), which was then inserted into the center of the quartz tube. Another crucible containing ~1.2 g Se powder was located at the upstream side of the tube. After evacuating the tube to ~5 $\times 10^{-3}$ Torr, flows of 40 sccm (standard cubic centimeter per minute) argon and 6 sccm hydrogen gas were introduced into the tube, and the reaction was conducted at 780 ºC (with a ramping rate of 30 ºC/min) for 5 min at a reaction chamber pressure of 20 Torr. At 780 ºC, the temperature at the location of Se powder was ~290 ºC. After growth, the furnace was cooled naturally to room temperature.

Flakes transfer and heterojunction fabrication. For the heterojunction fabrication and TEM sample preparation, poly(methyl methacrylate) (PMMA) was first spun onto the SiO_2/Si substrate with monolayer crystals at 3500 r.p.m for 60 s. The PMMA-coated substrate was then floated on 1 M KOH solution that etched silica epi-layer, leaving the PMMA film with the monolayer crystals floating on the solution surface. The film was transferred to deionized water for several times to remove residual KOH. For TEM samples, the washed film was scooped onto a Cu TEM grid covered lacey carbon. For heterojunction fabrication, the film with monolayer $MoSe_2$ was stacked onto the substrate with monolayer $Mo_{1-x}W_xSe_2$. The PMMA was removed by acetone and baking at 300 °C under ~30 Torr with Ar/H_2 (95%/5%) flowing for 2 h.

Device Fabrication. Electron beam lithography (FEI DB-FIB with Raith pattern writing software) was used for the device fabrication on monolayer $MoSe_2$, $Mo_{1-x}W_xSe_2$, and $MoSe_2$−$Mo_{1-x}W_xSe_2$ heterojunction. Firstly, a layer of PMMA 495A4 was spin-coated on the SiO_2 (250 nm)/Si substrate with flakes followed by a 180 °C bake. After pattern writing and development, a 10 nm layer of Ti followed by a 50 nm layer of Au was deposited using electron beam evaporation. Finally, well-defined source and drain electrodes were revealed using lift-off process with Acetone/IPA.

Characterizations. The morphologies and compositions of the monolayer $MoSe_2$ and $Mo_{1-x}W_xSe_2$ crystals were characterized using optical microscopy (Leica DM4500 P), SEM (Zeiss Merlin SEM), AFM (Bruker Dimension Icon AFM), Auger analysis, and TOF-SIMS.

Auger analysis was performed using a Phi680 Scanning Auger Nanoprobe. The Nanoprobe uses a field emission (Schottky) electron gun focused to approximately 15 nm in diameter. Auger electrons are energy analyzed using a double pass cylindrical mirror analyzer (CMA). Elemental maps were acquired using a 10 kV electron probe beam rastered over an area of 128 x128 pixels.

The atomic structures of monolayer $MoSe_2$ and $Mo_{1-x}W_xSe_2$ were investigated using aberration-corrected ADF-STEM (Nion UltraSTEM^{TM} 100) operating at 100 kV, using a half-angle range of the annular dark field detector with angles ranging from 86 to 200 mrad.

Raman measurements were performed using a micro-Raman system (JobinYvon Horiba, T64000) based on a triple spectrometer with three 1800 groves/mm gratings equipped with a liquid nitrogen cooled CCD detector. The Raman spectra were acquired under a microscope in backscattering configuration using 532 nm laser excitation (0.1mW laser power). The excitation laser was focused to a ~1 μm spot using a microscope objective (100x, N/A = 0.9).

PL measurements were conducted using a home-built micro-PL setup, which included an upright microscope coupled to a spectrometer (Spectra Pro 2300i, Acton, f = 0.3 m, 150 groves/mm grating) equipped with a CCD camera (Pixis 256BR, Princeton Instruments). The PL was collected through a 100x objective.

The band structures of monolayer $MoSe_2$ and $Mo_{1-x}W_xSe_2$ were analyzed using STM/S measurements, which were carried out in an Omicron variable temperature STM. All the measurements were performed at room temperature. Before STM investigations, samples were cleaned in-situ by heating them up to 200 °C for 2 hours. Topography images were taken in constant current mode. The differential conductance (dI/dV) was obtained by numerical differentiation of the I-V curves.

The μ-XPS measurements were carried out at scanning photoelectron microscopy (SPEM) endstation located at beamline 09A1 of National Synchrotron Radiation Research Center, Taiwan. The SPEM system equipped with a Fresnel zone plate optical system to focus soft X-ray down to 100 nm spot size. The samples were annealed at 200 °C prior to the experiments under ultrahigh vacuum condition. The photon energy was 400 eV for all μ-XPS measurements, which

was calibrated by the Au 4f core level signal emitted from a clean gold foil electrically connected with the samples.

The electrical properties of the monolayer flakes and heterojunctions were measured in vacuum (~10^{-6} Torr) in a probe station using a semiconductor analyzer (Keithley 4200). The mobility (μ) was calculated from the equation: $\mu = (L/WC_{ox})*(\Delta G/\Delta V_{bg})$, where L is the channel length, W the channel width, $G = I_{ds}/V_{ds}$ and $C_{ox} = 1.2\text{x}10^{-8}$ F/cm^2 (the capacitance between channel and the back gate per unit area, $C_{ox} = \varepsilon_0\varepsilon_r/d_{ox}$, $\varepsilon_0 = 8.85\text{x}10^{-12}$ F/m, $\varepsilon_r = 3.9$ and $d_{ox} = 300$ nm). The threshold voltage (V_{th}) was calculated from the transfer curve (I_{ds}–V_{bg}). The method was to draw the tangent line on the transfer curve across the point corresponding to the peak of the transconductance curve $g_m = \partial I_{ds}/\partial V_{bg}$, and the interception of the tangent line with x-axis is the threshold voltage.

Supporting figures

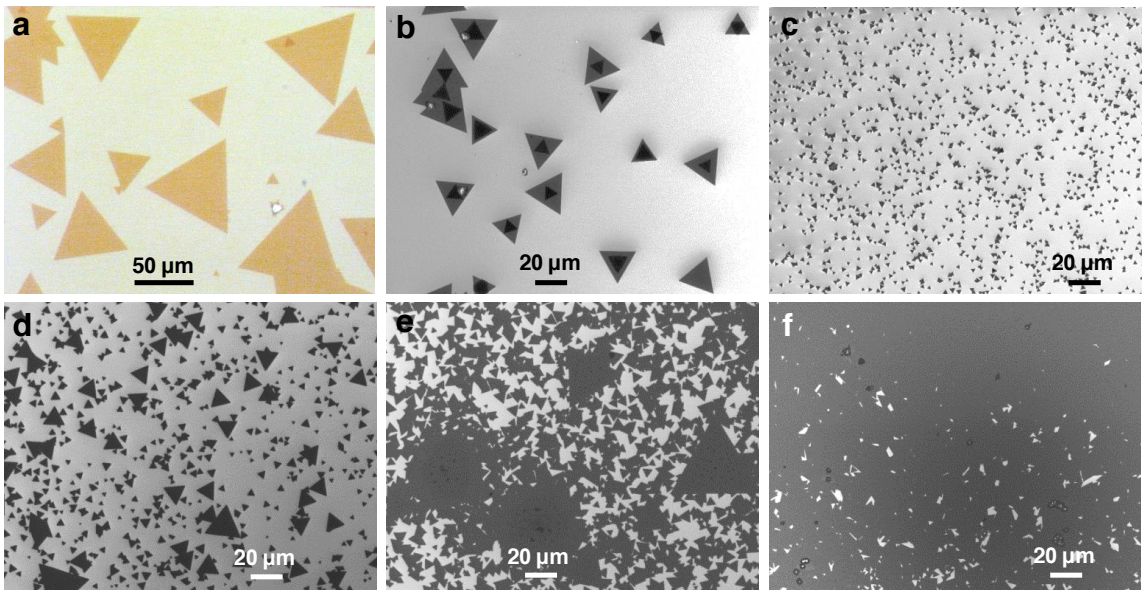

Figure S1. (**a**) Optical micrograph of monolayer $Mo_{1-x}W_xSe_2$. (**b**) SEM image of bilayer $MoSe_2$. (**c**) SEM image of monolayer $MoSe_2$ flakes grown when the substrate was placed face-up. (**d**–**f**) SEM images of monolayer $MoSe_2$ grown for 5 min, 10 min, and 15 min, respectively.

The layer number, size, and density of the $MoSe_2$ flakes can be controlled by growth conditions. With a typical growth condition as described in the Method (under 780 °C growth temperature, 40 sccm Ar, 6 sccm H_2, 20 Torr reaction chamber pressure for 5 min, and with the growth substrates placed face-down), large, uniform monolayer $MoSe_2$ flakes were obtained (Fig. S1a). When the reaction chamber pressure was increased to 30 Torr with other conditions being unchanged, many bilayer $MoSe_2$ flakes were obtained (Fig. S1b). Much smaller monolayer flakes were obtained if the substrates were placed face-up (Fig. S1c). As the growth time was increased, the density of the monolayer flakes increased, and individual triangular flakes merged into larger domains (Fig. S1d–f).

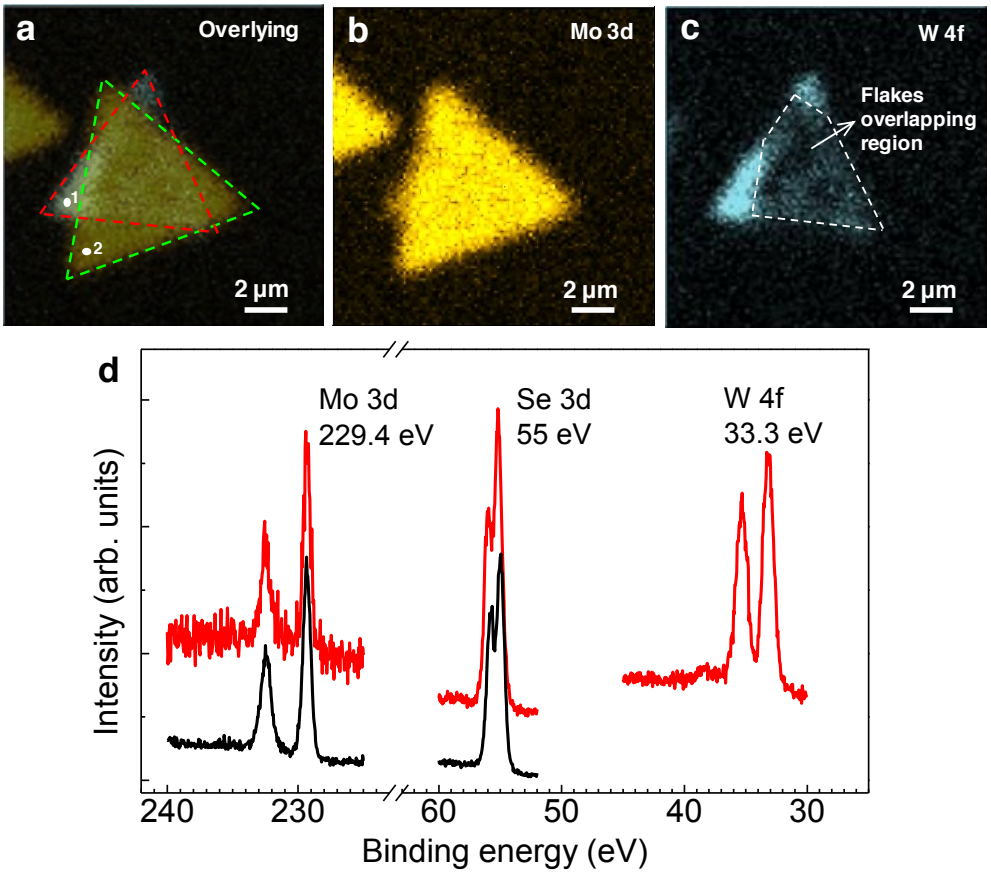

Figure S2. μ-XPS measurements on monolayer $MoSe_2$ and $Mo_{1-x}W_xSe_2$. (**a**–**c**) The Mo3d and W4f mappings for a monolayer $MoSe_2$ flaked transferred and stacked on a monolayer $Mo_{1-x}W_xSe_2$ flake. (a) is the overall mapping, with the green and red dashed triangles indicate the $MoSe_2$ (on top) and $Mo_{1-x}W_xSe_2$, respectively. (b) is the Mo3d mapping. (c) is the W4f mapping. (**d**) XPS spectra acquired from spot 1 (solid black curves) and spot 2 (solid red curves) shown in (a).

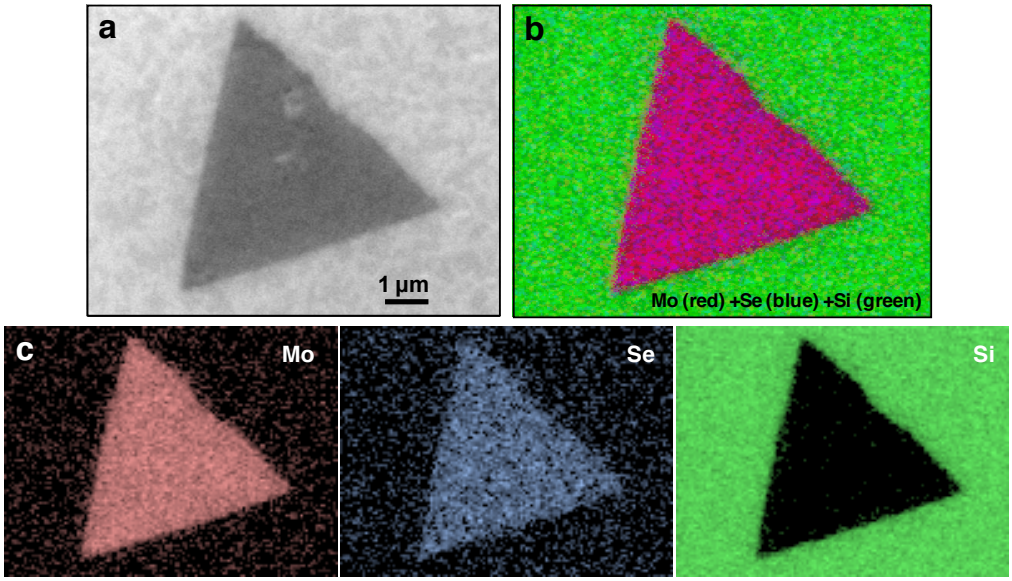

Figure S3. Nano-Auger mapping of monolayer $MoSe_2$. (**a**) SEM image of a monolayer $MoSe_2$ flake. (**b**) Nano-Auger elemental mapping of Mo, Se, and Si on the flake shown in (a). Si signal comes from the substrate as the background. (**c**) Color combination of Mo, Se, and Si maps in (b).

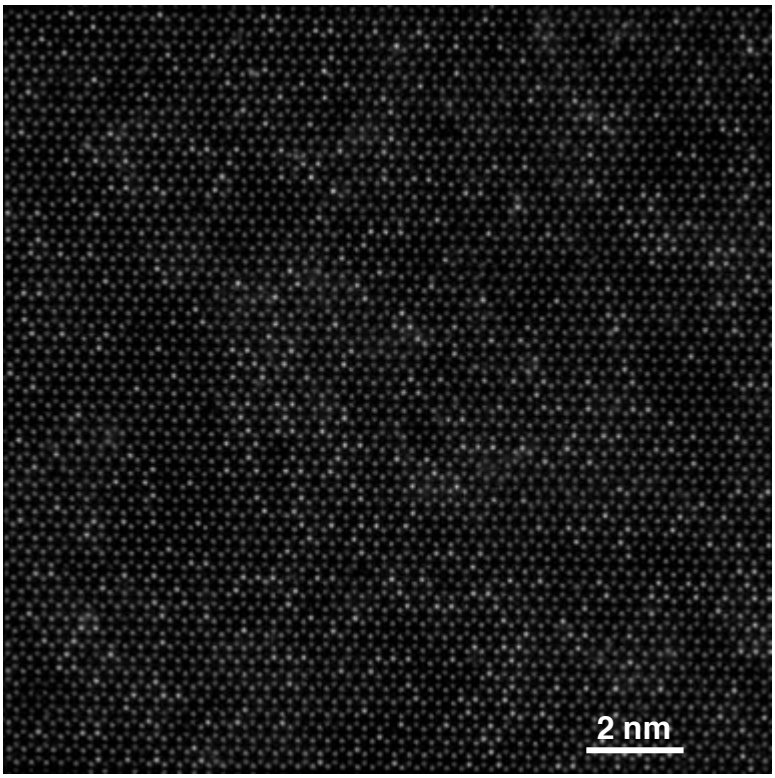

Figure S4. Atomic resolution ADF-STEM image in lower magnification of monolayer $Mo_{0.82}W_{0.18}Se_2$. According to statistic from the images, the W concentration is 18%, which is in good agreement with the results from other composition analysis.

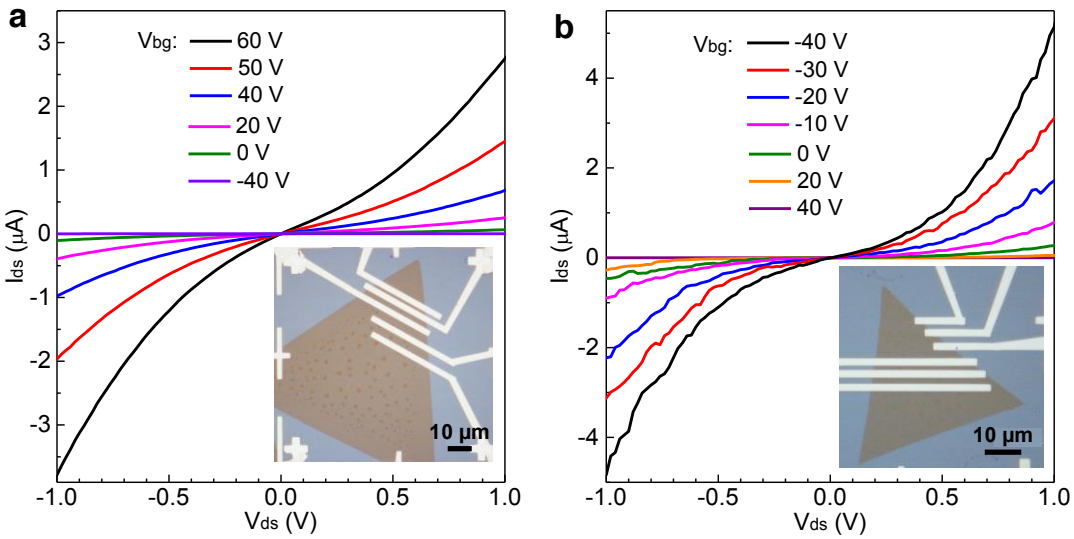

Figure S5. (**a**,**b**) Output (I_{ds}–V_{ds}) curves at different back-gate voltages of the monolayer $MoSe_2$ FET (a) and $Mo_{0.82}W_{0.18}Se_2$ FET (b). Insets of (a,b) are optical micrographs of corresponding FET devices.

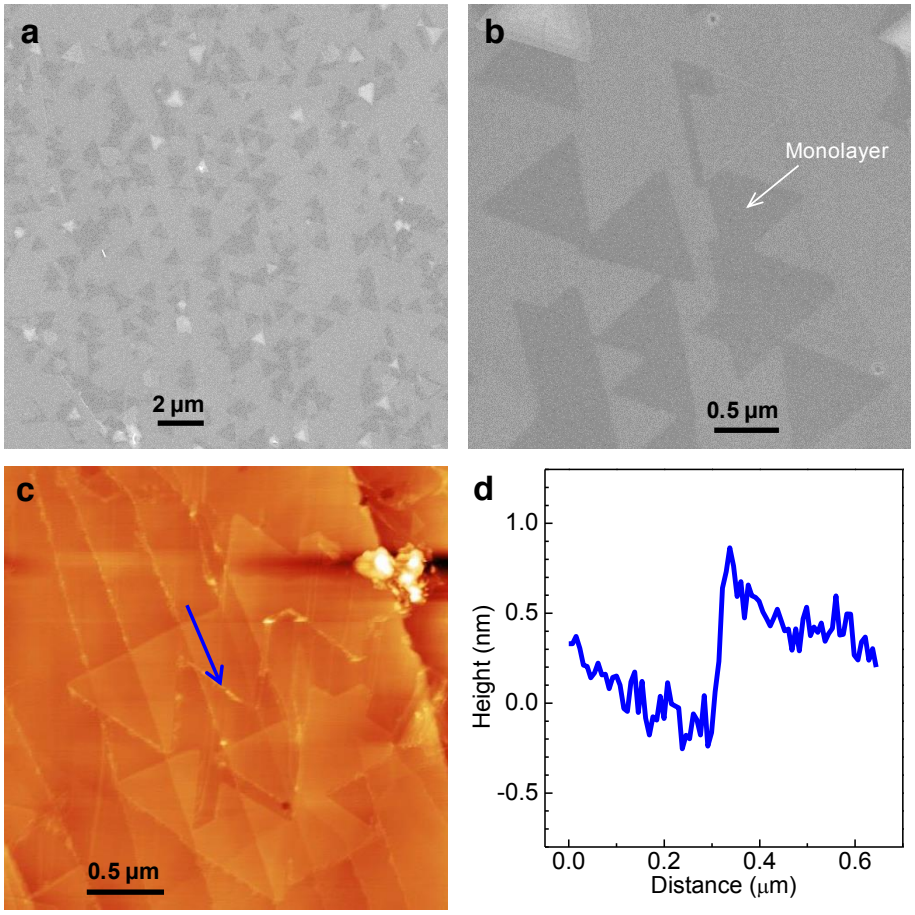

Figure S6. $Mo_{1-x}W_xSe_2$ flakes grown on HOPG. (**a**,**b**) SEM images of $Mo_{1-x}W_xSe_2$ flakes grown on HOPG. Most of the flakes are monolayer as indicated by the solid white arrow in (b). (**c**) AFM image of monolayer $Mo_{1-x}W_xSe_2$ flakes grown on HOPG. (**d**) Height profile along the solid blue arrow in (c).

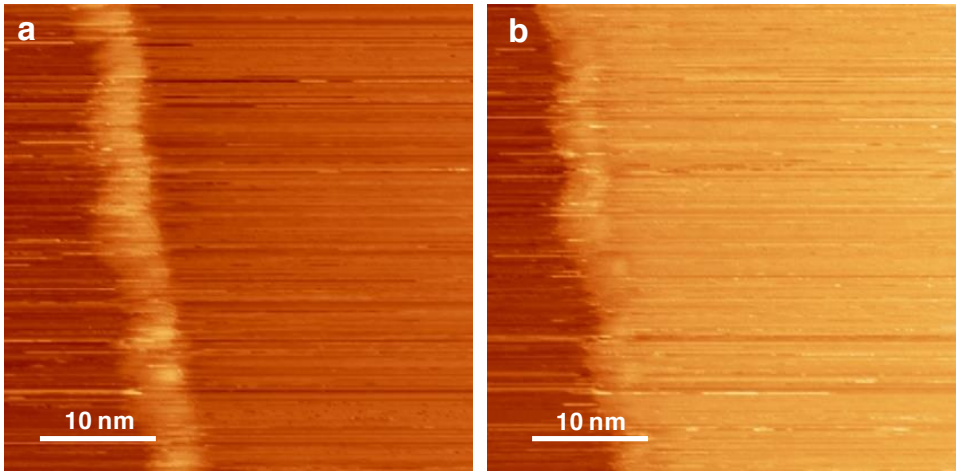

Figure S7. Low magnification STM images obtained from pure monolayer $MoSe_2$ grown on HOPG with V = -1 V, I = 50 pA (**a**) and V = 1 V. I = 50 pA (**b**).